The Role of Ocean in the Response of Tropical Climatology to Global Warming: The West–East SST Contrast

ZHENGYU LIU

Department of Atmospheric and Oceanic Sciences, University of Wisconsin—Madison, Madison, Wisconsin

(Manuscript received 30 September 1996, in final form 31 July 1997)

ABSTRACT

A theory of tropical climatology is used to study the role of ocean in the response of tropical climatology to global warming. Special emphasis is given to the response of the west–east SST contrast along the equator. The transient response of tropical sea surface temperature to a global warming is shown to have two distinctive stages: a fast surface adjustment stage of years and a slow thermocline adjustment stage of decades.

Under a global warming heat flux that does not vary much in space, the initial response is always an enhanced west–east SST contrast. The final equilibrium response, however, depends on the effective latitudinal differential heating. The west–east SST contrast increases for an enhanced latitudinal differential heating, and vise versa.

1. Introduction

Recent attempts toward the understanding of the response of tropical climatology to global warming have promoted a growing interest on tropical climatology from observations (Ramanathan and Collins 1991; Wallace 1992; Fu et al. 1992; Hartmann and Michelsen 1993; Waliser 1996), coupled ocean–atmosphere models (Meehl and Washington 1989, 1996; Knutson and Manabe 1995), and theories (Neelin and Dijkstra 1995; Dijkstra and Neelin 1995; Pierrehumbert 1995; Sun and Liu 1996; Clement et al. 1996; Liu and Huang 1997; Seager and Murtugudde 1997; Miller 1997). Most of the studies so far have focused on the warming magnitude of tropical SST.

The other equally important aspect of the response of tropical climatology is the spatial pattern, which could provide a powerful fingerprint of global warming detection. Recent observational analyses seem to suggest an increased west–east SST contrast of a few tenths of a degree in the central equatorial Pacific during the last century (Cane et al. 1997; Kaplan et al. 1998; Latif et al. 1997). This observed increase of SST contrast is difficult to interpret in terms of most existing mechanisms on tropical SST, such as temperature–evaporation feedback, cloud–albedo feedback, and the atmospheric heat transport, all of which tend to give a reduced west–east SST contrast with a global warming. Therefore, one of our major motivations is to understand how a west–east SST contrast can be increased under a global warming.

In a recent study, Clement et al. (1996) (hereafter CSCZ) proposed a mechanism for the increased zonal SST gradient under a spatially uniform global warming over the ocean. The warm pool is dominated by the local surface heat flux, while the cold tongue is strongly controlled by the cold upwelling. As a result, an increase of surface heat flux uniformly over the Tropics results in a warming that is stronger in the warm pool than in the cold tongue. This mechanism is a local mechanism that is independent of the extratropics. This mechanism, however, seems to be inconsistent with the study of Liu and Huang (1997, hereafter LH) who have shown that in the final steady equilibrium state, the west–east SST contrast, is determined by the latitudinal differential heating. The understanding of this inconsistency provides another major motivation of this work.

It will be shown that the local mechanism of CSCZ is a transient mechanism that is most effective at interannual timescales. At an interdecadal timescale, which is the adjustment timescale of the thermocline circulation, the west–east SST contrast is determined by the latitudinal differential heating (more accurately, the latitudinal difference of local-equilibrium SSTs) as proposed by LH. This equilibrium mechanism, in contrast to that of CSCZ, is a nonlocal mechanism that depends critically on the extratropical climate conditions.

In a special, yet important case of a spatially uniform surface heat flux warming, an enhanced west–east SST contrast can be sustained at the final equilibrium (Seager and Murtugudde 1997, hereafter SM). This occurs because the surface heat flux sensitivity to perturbation SST increases away from the equator mainly due to the

Corresponding author address: Z. Liu, Dept. of Atmospheric and Oceanic Sciences, 1225 W. Dayton St., University of Wisconsin—Madison, Madison, WI 53706-1695.
E-mail: znl@ocean.meteor.wisc.edu

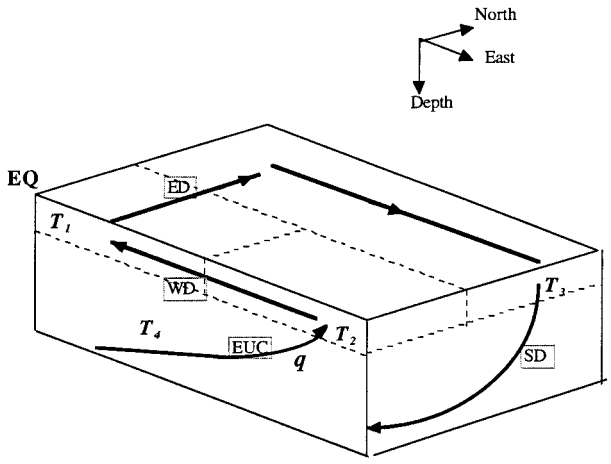

FIG. 1. Schematic figure for the four-box ocean model. The surface Pacific equator is represented by surface western box and eastern box respectively, with the temperatures of T_1 and T_2, respectively. The surface midlatitude ocean is represented by the third box with the temperature of T_3. The midlatitude thermocline is combined with the equatorial thermocline as a subsurface thermocline box with a temperature of T_4. Major ocean currents are labeled as EUC for Equatorial Undercurrent and upwelling, WD for surface westward wind drift, ED for poleward Ekman drift, and SD for subduction flow (see LH for more discussions).

increased wind speed and in turn evaporation. Therefore, a uniform surface heat flux tends to warm the SST less in the extratropics, which increases the latitudinal SST difference and in turn the zonal SST contrast.

It should be pointed out that, since our focus on the oceanic processes, we have chosen not to include explicit atmospheric processes. One should therefore be cautious in directly relating our results to the study of realistic CO_2 increase. The paper is arranged as follows. Section 2 will extend our previous model to include more general surface heat flux conditions. This will allow us to study the increased west–east SST contrast under a uniform surface heat flux. Section 3 will investigate the transient oceanic response to a global warming forcing, which illustrates the transient nature of the local mechanism of CSCZ. Further discussions are given in section 4.

2. Equilibrium response to global warming: The nonlocal mechanism

a. The box model

Following LH, the tropical–extratropical upper ocean will be represented by four boxes: box 1, 2, 3, and 4, representing the surface warm pool, cold tongue, the extratropical surface ocean, and the subsurface thermocline, respectively (Fig. 1; see LH for more details). The temperatures of the four boxes will be represented by T_1^*, T_2^*, T_3^*, and T_4^*. The extratropical–tropical upper-ocean circulation consists of the westward wind drift, the poleward Ekman drift, the equatorward thermocline subduction, and the eastward Equatorial Undercurrent. This tropical–extratropical circulation will be seen of fundamental importance to both the transient and equilibrium responses of the tropical climatology to a global warming.

The tropical–extratropical exchange transport is q^*, and the surface heat fluxes per unit area are F_n ($n = 1$, 2, 3). We therefore have the heat budget for the four ocean boxes as

$$c_P\rho h_1 A_1 dT_1^*/dt = A_1F_1 + c_P\rho q^*(T_2^* - T_1^*), \quad (2.1a)$$

$$c_P\rho h_2 A_2 dT_2^*/dt = A_2F_2 + c_P\rho q^*(T_4^* - T_2^*), \quad (2.1b)$$

$$c_P\rho h_3 A_3 dT_3^*/dt = A_3F_3 + c_P\rho q^*(T_1^* - T_3^*), \quad \text{and} \quad (2.1c)$$

$$c_P\rho h_4 A_4 dT_4^*/dt = c_P\rho q^*(T_3^* - T_4^*). \quad (2.1d)$$

It is interesting to notice that the depths of surface mixed layers (which also crudely represent the depth of thermocline in the equatorial region) do not affect the final steady-state solution, although it can affect the transient evolution. A shallower mixed-layer depth gives a small volume of water, which is changed more by the surface flux forcing. In the mean time, however, a smaller volume is also affected more by the heat transport. In other words, the depth of the mixed layer does not change the relative strength of surface flux and heat transport in the box model.[1]

The surface heat flux will be approximated as $F_n(T_n^*) = F_n(T_0) + (T_n^* - T_0)\partial_T F_n$, $n = 1$, 2, 3, where $\partial_T F_n$ (<0) represents the heat flux sensitivity to perturbation SST due to local negative air–sea feedback and is estimated at a reference temperature T_0. Rewrite the heat flux in the restoring form: $F_n = (T_{n\mathrm{R}} - T_n^*)|\partial_T F_n|$; the restoring temperatures can be written as

$$T_{n\mathrm{R}} = T_0 + F_n/|\partial_T F_n|. \quad (2.2)$$

The restoring temperature equals the *local-equilibrium* SST, which will be reached in the absence of ocean currents. It may be regarded crudely as the radiative–convective–equilibrium SST in the coupled ocean–atmosphere system (Sun and Liu 1996).[2] To focus on the west–east asymmetry due to oceanic processes, we will use the same local-equilibrium SSTs for the two equatorial boxes: $T_E = T_{1\mathrm{R}} = T_{2\mathrm{R}}$. A cooler midlatitude local-equilibrium SST T_M ($<T_E$) will be imposed to simulate the latitudinal differential heating to the ocean.

Equation (2.1) can be written in the nondimensional form as

[1] It is, however, possible that different mixed-layer depths can affect the stratification and in turn the heat transport in more realistic models.

[2] Strictly speaking, the effect of atmospheric dynamics is included. The local-equilibrium SST can in principle be obtained from the equilibrium SST in a full AGCM coupled with a slab mixed layer.

$$dT_1/d\tau = 1 - T_1 + q(T_2 - T_1), \quad (2.3a)$$

$$m_2 dT_2/d\tau = r_2[(1 - T_2)/\tau_2] + q(T_4 - T_2), \quad (2.3b)$$

$$m_3 dT_3/d\tau = r_3(-T_3/\tau_3) + q(T_1 - T_3), \quad \text{and} \quad (2.3c)$$

$$m_4 dT_4/d\tau = q(T_3 - T_4), \quad (2.3d)$$

where we have used the dimensionless temperature, time, restoring time, and transport as $T_n = (T_n^* - T_M)/(T_E - T_M)$ $(n = 1, 2, 3, 4)$, $\tau = t/t_1$, $\tau_n = t_n/t_1$ $(n = 2, 3)$, and $q = q^*\tau_1/h_1A_1$, respectively. In addition, $m_n = h_nA_n/h_1A_1$ $(n = 2, 3, 4)$ are the ratios of the volume of each box to that of box 1, and $r_n = A_n/A_1$ $(n = 2, 3)$ are the ratios of the surface area of each box to that of box 1. The dimensional restoring times

$$t_n = c_P\rho h_n/|\partial_T F_n|, \qquad n = 1, 2, 3, \quad (2.4)$$

represent the strength of the local negative air–sea feedback and are at the order of a year for a mixed layer of 50 m (e.g., Bretherton 1982; Seager et al. 1995; Lau and Nath 1996; Sun and Liu 1996). Since the climate condition along the equator is rather uniform relative to that between the equator and the extratropics, at the first order, we assume that the warm pool and cold tongue have the same mixed-layer depths, areas, and restoring times: $h_1 = h_2$, $A_1 = A_2$, $t_1 = t_2$, which lead to $\tau_2 = 1$, $m_2 = r_2 = 1$.[3] Equations (2.3) therefore reduce to

$$dT_1/d\tau = 1 - T_1 + q(T_2 - T_1), \quad (2.5a)$$

$$dT_2/d\tau = 1 - T_2 + q(T_4 - T_2), \quad (2.5b)$$

$$mdT_3/d\tau = -mT_3/\tau_3 + q(T_1 - T_3), \quad \text{and} \quad (2.5c)$$

$$MdT_4/d\tau = q(T_3 - T_4), \quad (2.5d)$$

where we have assumed a midlatitude mixed-layer depth the same as that in the Tropics, so that $r_3 = m_3$. In addition, we use the notation $m \equiv m_3$ and $M \equiv m_4$, which have typical values of $m >$ or $\sim O(1)$ and $M \gg 1$ in a realistic ocean.

b. Equilibrium response to global warming

We now consider the final steady-state response of west–east SST contrast to a global warming. First, we give a brief review of the steady-state solution of (2.5) (see LH for more details). The major result is that the west–east SST difference is regulated by ocean currents below an upper bound that is about a quarter of the meridional difference of local-equilibrium SSTs. For the purpose here, we only discuss a simple case in which the extratropical ocean is much larger than the tropical ocean ($m = \infty$). The steady-state solution has the west–east SST difference[4] as $T_1 - T_2 = q/(1 + q)^2$, or in dimensional SSTs and surface heat fluxes as

$$T_1^* - T_2^* = \frac{q}{(1 + q)^2}(T_E - T_M) = \frac{q}{(1 + q)^2}\left(\frac{F_E}{|\partial_T F_E|} - \frac{F_M}{|\partial_T F_M|}\right), \quad (2.6)$$

where we have used $T_E = F_E/|\partial_T F_E|$ $(= F_1/|\partial_T F_1| = F_2/|\partial_T F_2|)$ in the Tropics and $T_M = F_M/|\partial_T F_M|$ $(= F_3/|\partial_T F_3|)$ in the extratropics. A global warming climate forcing to the ocean can be simulated as anomalous surface heat fluxes δF_E in the Tropics and δF_M in the midlatitude. The change of west–east SST contrast is then

$$\delta(T_1^* - T_2^*) = \frac{q}{(1 + q)^2}(\delta T_E - \delta T_M) = \frac{q}{(1 + q)^2}\left(\frac{\delta F_E}{|\partial_T F_E|} - \frac{\delta F_M}{|\partial_T F_M|}\right), \quad (2.7)$$

where

$$\delta T_E = \delta F_E/|\partial_T F_E|, \qquad \delta T_M = \delta F_E/|\partial_T F_M| \quad (2.8)$$

are the corresponding anomalous local-equilibrium SSTs in the Tropics and midlatitude, respectively. It is clear from (2.6) or (2.7) that the west–east SST contrast at the final equilibrium is determined completely by the latitudinal difference of local-equilibrium SSTs.

It is, however, important to notice that the local-equilibrium SST depends on not only the surface heat flux, but also the surface heat flux sensitivity to perturbation SST, as seen in (2.2) and (2.8). If the surface heat flux sensitivity is not much different between the equator and the extratropics, a stronger surface heat flux along the equator will result in a stronger warming of local-equilibrium SST there. The increased latitudinal difference of local-equilibrium SST will eventually increase the west–east SST contrast.

However, the surface heat flux sensitivity is significantly stronger (over 60%) in the midlatitude than in the equatorial region, as studied by Seager et al. (1995) with an atmospheric boundary layer model and by Lau and Nath (1996) with an AGCM. This is mainly caused by the stronger surface wind and in turn evaporation in the midlatitude. This stronger heat flux sensitivity has been shown important for the regulation of basin-mean SST (SM) because it makes the midlatitude an efficient radiator-fin to loss heat. A similar conclusion has also been drawn from the atmospheric point of view by Pierrehumbert (1995).

Here, we also see that the stronger heat flux sensitivity

[3] For example, the surface heat flux sensitivity increases by no more than 20% from west to the east in the equatorial Pacific, but can increase by over 70% toward the midlatitude (Seager et al. 1995; Lau and Nath 1996). A relevant discussion can also be found in footnote 4.

[4] This is not very sensitive to the west–east difference of climate conditions. For example, for a general τ_2 [using (2.3)], we will have $T_1 - T_2 = \tau_2 q/(1 + q)(1 + \tau_2 q)$. For a τ_2 change of 50%, the upper bound of $T_1 - T_2$ changes by about 30%.

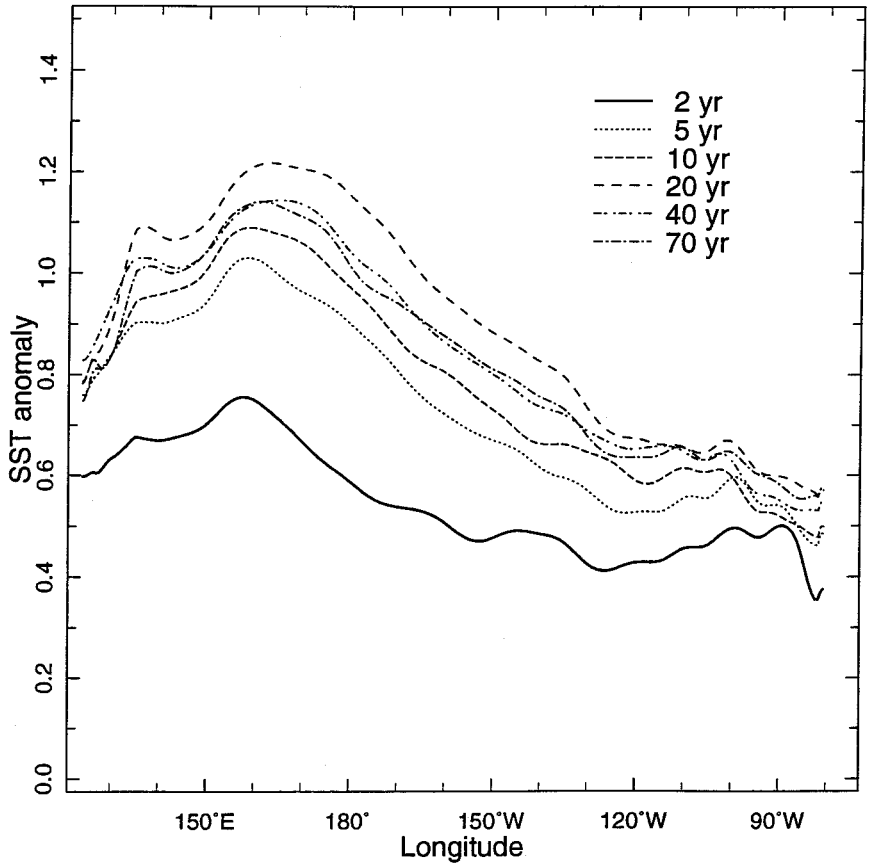

FIG. 2. Results from an ocean circulation model simulation of Seager and Murtugudde (1997) with fixed winds and a realistic surface heat flux formulation to which a uniform heating of 10 W m^{-2} has been added. Changes from the initial state in SST gradient along the equator is shown for years 2 (solid line), 5 (dotted), 10 (dashed), 20 (dashed with blanks), 40 (dashed dot with blanks), and 70 (dashed dot). Most of the adjustment takes place in the first 2 yr, and the steady state is closely approached by year 40 [after Cane et al. (1997)].

can affect the west–east SST contrast significantly. A special, yet important case, which may be relevant to global warming, is a uniform surface heat flux forcing. The higher surface heat flux sensitivity reduces the warming of SST in the extratropics compared with that in the Tropics. Therefore, this anomalously cold equatorial source water will eventually also reduce the warming of the eastern cold tongue SST after the thermocline circulation timescale. The west–east SST contrast will therefore be increased at the final equilibrium. This has been discussed by SM in their OGCM experiments.

Here, we can further give a quantitative estimate of the change of west–east SST contrast. For a uniform surface heat flux warming $\delta F_E = \delta F_M \equiv \delta F$, we have from (2.7) that

$$\delta(T_1^* - T_2^*) = \frac{q}{(1+q)^2}\delta T_E\left(1 - \frac{\partial_T F_E}{\partial_T F_M}\right) \leq \frac{\delta T_E}{4}\left(1 - \frac{\partial_T F_E}{\partial_T F_M}\right). \quad (2.9)$$

Adopting a ratio of heat flux sensitivity of $\partial_T F_E/\partial_T F_M \approx 60\%$ (Seager et al. 1995; Lau and Nath 1996), we have from (2.9) the estimate of the upper bound of the change of west–east SST contrast as

$$\delta(T_1 - T_2) \approx \delta T_E/10. \quad (2.10)$$

The Pacific tropical climatology has been estimated to be close to the upper-bound state (or the so-called saturation state) (see LH; Liu 1997). Therefore, (2.10) gives a first-order approximation in the Pacific under a uniform global surface heat flux. For an anomalous heat flux of $\delta F = 10$ W m^{-2} and a tropical sensitivity of $\partial_T F_E = 4$ W m^{-2} K^{-1} (Seager et al. 1995), the increase of tropical local-equilibrium SST is about $\delta T_E = 2.5$ K according to (2.8), and the increase of west–east SST difference $\delta(T_1 - T_2)$ is about 0.25 K according to (2.10). This can explain about 70% of the change in the OGCM simulation of SM. Figure 2 [from Cane et al. (1997)] shows the response of the equatorial SST under a 10 W m^{-2} uniform surface heat flux forcing in an ocean general circulation model that is coupled to the

atmospheric boundary layer model of Seager et al. (1995). The averaged SST contrast between the western and eastern equatorial region is increased by about 0.35 K in the final equilibrium state. It should be noticed that (2.10) still seems to underestimate the increase of west–east SST contrast. Additional increase of zonal SST contrast may be caused by a stronger heat flux sensitivity in the east than the west (Seager et al. 1995), as well as the high-latitude effect (see section 4).

Finally, one may notice another effect of the surface heat flux sensitivity on the zonal SST contrast. In a realistic case where the extratropics are not very large ($m < \infty$), (2.5c) shows an explicit dependence on τ_3. However, for steady state, τ_3 can be combined with the extratropical area ratio parameter m: a decrease in τ_3 is equivalent to an increase of m (and vise versa). It has been shown in LH that the steady-state west–east SST contrast is not very sensitive to m in the regime of realistic parameters. Therefore, this effect seems to be not important for the west–east SST contrast.

3. Transient response to global warming

The nonlocal equilibrium mechanism discussed above differs substantially from the local mechanism of CSCZ. The relationship between the two mechanisms will become clear in the following study, which will focus on the transient response of ocean to a global warming. We will first study the box model (2.5) and later an OGCM. In this section, unless otherwise specified, we will use local-equilibrium SST, instead of surface heat flux, as the climate forcing, since we are now not interested in the spatial variation of heat flux sensitivity. Accordingly, $\tau_3 = 1$ is also set in (2.5).

a. Response to a sudden onset of global warming

To illustrate the nature of the mechanism of CSCZ more clearly, a sudden onset of a global warming that increases toward the extratropics ($\delta T_E = 0.2$ and $\delta T_M = 0.4$) will be imposed. According to (2.6), this heating forcing reduces latitudinal differential heating and therefore should reduce the west–east SST contrast at the final steady state.

However, the west–east SST contrast $T_1 - T_2$ increases in the initial stage (about $t < 3$) as shown in Fig. 3b. This increase occurs because the SST increases faster in the warm pool T_1 than in the cold tongue T_2 (Fig. 3a). As suggested by CSCZ, the warm pool is controlled more by the surface heat flux, while the cold tongue is strongly affected by the cold oceanic upwelling. The same surface heat flux anomaly therefore warms the warm pool faster than the cold tongue. This initial surface adjustment stage is dominated by the rapid surface processes, including the local thermodynamic interaction and surface advection.

In spite of the initial increase of west–east SST contrast at the interannual timescale, the west–east SST contrast eventually decreases at the interdecadal timescale, lasting to the final steady state with a zonal SST difference smaller than that of the initial state as shown in (2.6). However, the reduction of SST contrast is opposite to that from CSCZ. This occurs because the tropical–extratropical thermocline feedback is absent in the intermediate model of CSCZ. This later thermocline adjustment stage is dominated by slow subsurface ocean circulation, which adjusts at interdecadal timescales.

It is also interesting to observe in Fig. 3b the unique

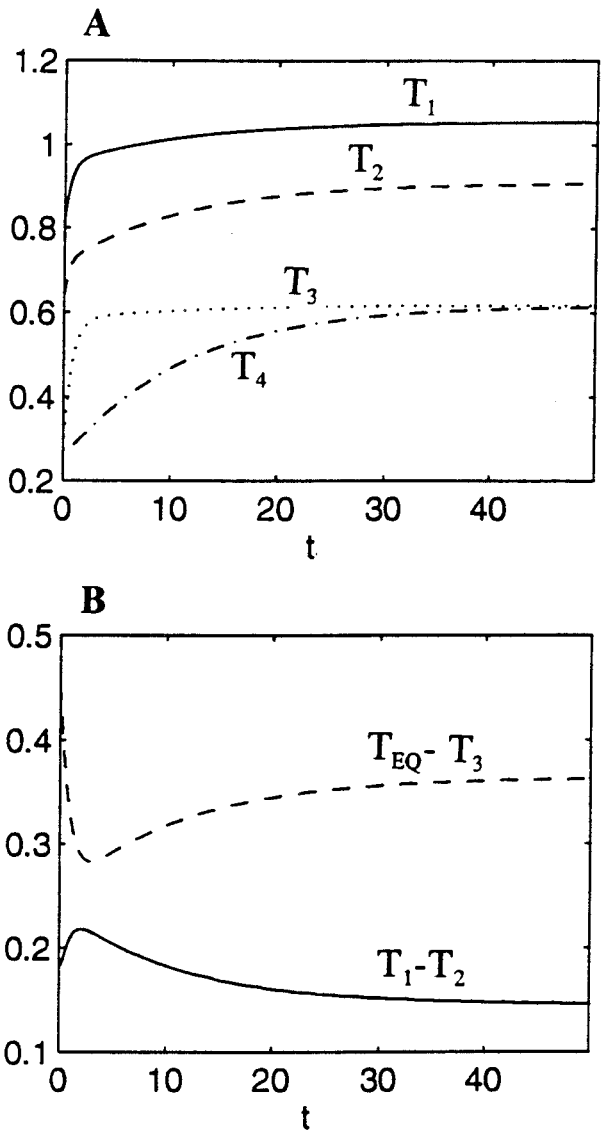

FIG. 3. The temporal evolution of the response of the box model (2.5) to a sudden onset of global warming with $\delta T_E = 0.2$ and $\delta T_m = 0.4$. (a) Temperatures in each box, (b) zonal ($T_1 - T_2$) and meridional SST [$T_{EQ} - T_3$, where $T_{EQ} = 0.5(T_1 + T_2)$] differences. The box model parameters are ($q = 1$, $m = 2$, $M = 10$, and $\tau_3 = 1$). It shows clearly the two stages of responses. The zonal SST gradient first intensifies but later returns to its new (and weaker) equilibrium state. The opposite phase between the zonal and meridional SST gradient is also clearly seen.

transient behavior of the latitudinal SST difference $T_{EQ} - T_3$, which shows virtually an out-of-phase relationship with the zonal SST difference $T_1 - T_2$ along the equator. This negative correlation is caused by the heat exchange between the Tropics and the extratropics. A uniform global warming imposes the same surface heating to all three surface boxes. The extratropics (T_3), however, receives an additional heat import due to the Ekman flow from the Tropics and therefore warms up the fastest (Fig. 3a). This tends to reduce the latitudinal SST gradient, opposite to the increased zonal SST gradient along the equator. Since the midlatitude SST has rapidly approached its final equilibrium in the initial stage, it remains virtually unchanged in the later thermocline adjustment stage (Fig. 3a). The equatorial SSTs, delayed by the cold thermocline water, still exhibits a slow warming trend (Fig. 3a). As a result, the trend of the latitudinal SST gradient is reversed.

We can understand the evolution of both the zonal and latitudinal SST gradients from a unified point of view. The cold extratropical thermocline subduction water reaches first the cold tongue, then the warm pool, and finally returns back to the extratropics. Thus, the influence of the negative thermocline feedback is the strongest on the cold tongue, weaker on the warm pool, and the weakest on the extratropics. This, under a uniform heating, results in a warming: the fastest in the extratropics, slower in the warm pool, and the slowest in the cold tongue. It is this nonuniform response that produces the evolution characteristics of both the zonal and meridional SST gradients. A long thermocline memory is crucial in allowing the different timescales of SST response to fully develop in different regions. The negative out-of-phase relation between the zonal and meridional SST gradients is therefore a transient effect. Indeed, in the final equilibrium state, one can easily show that the zonal and meridional SST contrasts are always in phase (see appendixes A and B for more details).

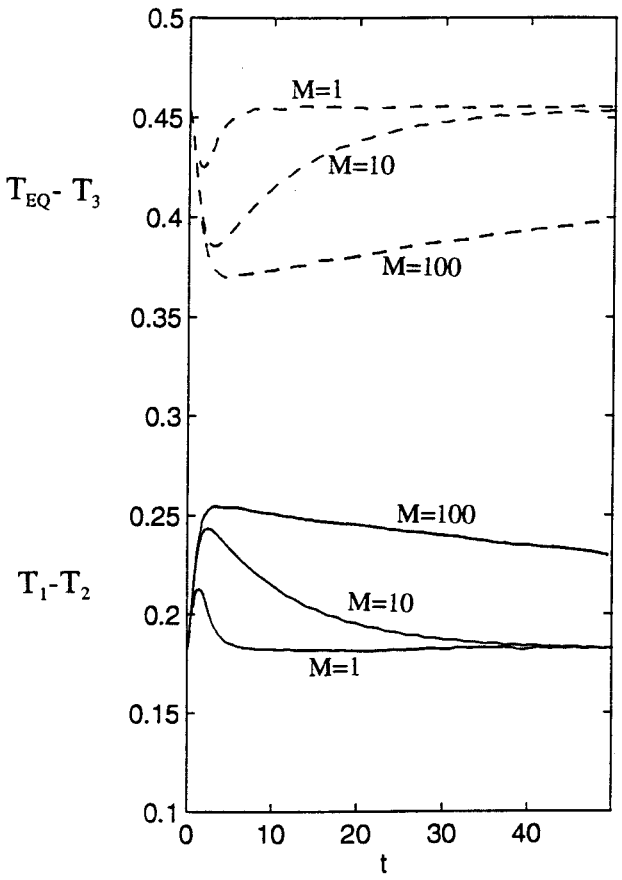

FIG. 4. The response of the box model to the sudden onset of a spatially uniform global warming of $\delta T_E = \delta T_m = 0.3$, for the zonal (solid) and meridional (dashed) SST differences with different subsurface water mass parameter *M*. Other parameters are the same in Fig. 3. The most important point is that the amplitude and adjustment time increases with the subsurface memory.

b. The role of thermocline memory

The thermocline memory, which is represented by the parameter *M*, can be shown crucial in determining both the timescale and the amplitude of the transient response (appendixes A and B), although *M* has no effect on the final equilibrium state [see (2.5) or LH]. Figure 4 shows three runs forced by a sudden onset of global warming $\delta T_E = \delta T_M = 0.3$ for different *M*. According to (2.6) or (2.7), the west–east SST contrast will not change in the final steady state. However, as in Fig. 3, the transient evolution of SST (Fig. 4) exhibits two distinct stages in both the zonal and meridional SST differences.

The most important feature in Fig. 4 is a smaller amplitude and a shorter adjustment time of the transient response for a decreased thermocline memory *M* (see appendix B for more general cases). This can be understood as follows. A small volume of subsurface water mass adjusts rapidly to the anomalous subduction heat transport. This enables the negative subsurface oceanic feedback to damp the SST anomaly quickly. On the other hand, with a large subsurface water mass, the amplitude of the response seems to saturate in Fig. 4. This occurs because the response approaches the equilibrium response that is discussed by LH but at a very slow subsurface advection time. The timescale of the initial surface adjustment stage is affected little, however, because it is determined mainly by the surface relaxation and surface advection.

Finally, the upper bound of the amplitude of the transient response can be derived from (B1a) (and the discussion that follows) as

$$\delta(T_1 - T_2) \le \delta T_E/4, \quad \textit{for transient response} \quad (3.1)$$

with the upper bound reached at the limit of large *M* and near saturation mean state of $q = 1$. This can be seen clearly in Fig. 4. Now, $\delta T_E = 0.3$. The maximum initial increase of west–east SST contrast (for $M = 100$ at $\tau \approx 2$) is about 0.7, which reaches the upper bound

of (3.1). A comparison between the transient response upper bound (3.1) and the steady-state response (2.9) also shows a striking similarity. Physically, the analogy can be stated this way: The transient response is caused by the temporal variability of the climate forcing, while the equilibrium response is caused by the spatial variability of the forcing (see appendixes A and B for more discussions).

c. Response to a transient global warming

A more realistic scenario is a gradually increased global warming forcing. Since the fast surface adjustment response of CSCZ occurs mainly at the interannual timescale, while the slow thermocline adjustment response occurs at interdecadal timescales. One can expect that the variability due to the fast surface adjustment weakens when the timescale for the transient global warming increases. This is shown in Fig. 5, where three transient global warming forcings are used. The global warming forcing of δT_E and δT_M increase linearly to the same level as in Fig. 3 in $t_H = 2$, 10, and 40, respectively, and remains unchanged thereafter (Fig. 5a). The evolution of the SST gradients for the fast warming case ($t_H = 2$ in Fig. 5b) is almost the same as the sudden global warming case (Fig. 3b). As the global warming becomes more gradual (decadal $t_H = 10$ case), the strengthening of the zonal SST difference is slowed, and the magnitude of the transient response is reduced. If the global warming is comparable to the thermocline adjustment time (multidecadal $t_H = 40$) here, the initial intensification of zonal SST difference almost disappears. Instead, the zonal SST difference remains almost unchanged for decades before it shows a significant decrease. Thus, for a slow global warming forcing, the fast surface adjustment response may not be excited significantly. The transient response will be a quasi-equilibrium response. This is also true for the meridional SST gradient. As a result, the zonal and meridional SST gradients are roughly in phase in the slow warming case, opposite to the two faster warming cases, which are dominated by surface adjustment and the related transient responses.

d. OGCM study

The box model results have been further substantiated by OGCM experiments. The OGCM is the GFDL MOM1, and the experiments are similar to the ocean-alone experiments in LH. Numerous experiments have been performed, including experiments with doubled resolution (see LH). Here we only show one experiment, which has a resolution of $4° \times 4° \times 15$ levels, a model domain of (0°, 60°) × (50°S, 50°N) × (0 m, 3000 m) and a surface-layer thickness of 20 m. The ocean is first spun up for 2000 yr forced by a uniform easterly wind stress of -0.5 dyn cm^{-2} and a restoring SST that increases linearly from −15°C on latitude 50° to 36°C on the equator. The restoring time is 100 days. The SST in the final equilibrium exhibits a typical tropical SST pattern with a broad warm pool in the west and a narrow cold tongue in the east and a zonal SST difference of about 4°C.

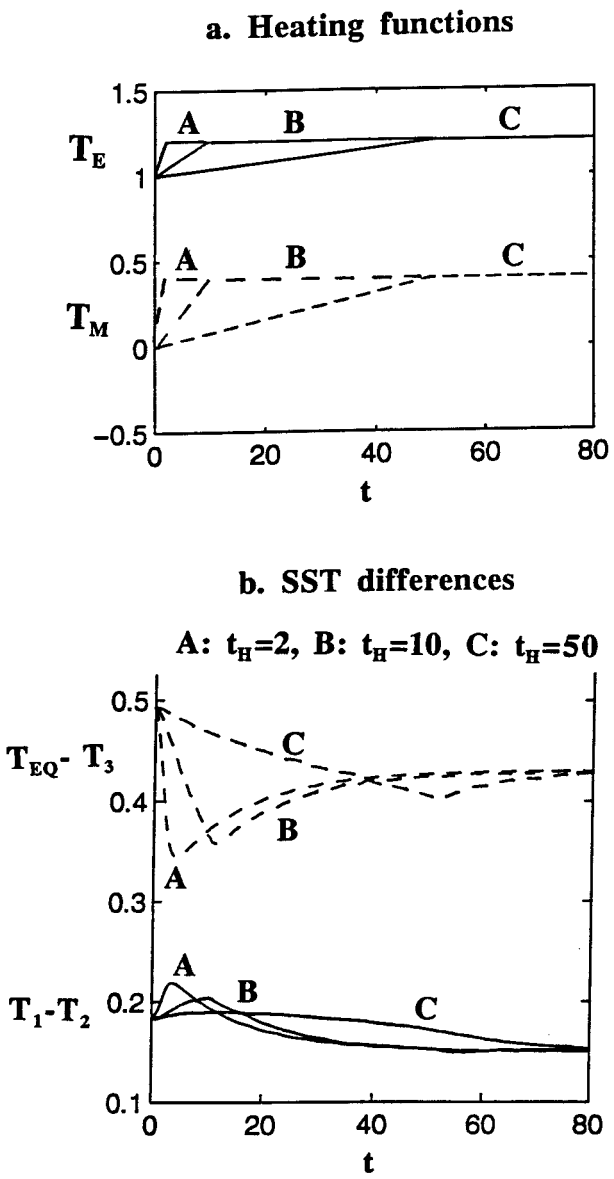

FIG. 5. Similar to Fig. 3 but for three transient global warming forcings, which has the initial linear transient time of 2 (curve A), 10 (curve B), and 50 (curve C), respectively. (a) The time series of the equilibrium SSTs (T_E solid and T_M dashed). (b) The zonal (solid) and meridional ($T_{EQ} - T_3$, dashed) SST differences. For a global warming of multidecadal timescales (curve C), the initial intensification of the zonal SST gradient almost vanishes. The other difference from Fig. 3 is that this is a coupled run with the coupled ocean current given by $q = A_W(T_1 - T_2) + A_H(T_{EQ} - T_3)$ where $A_W = 1$ and $A_H = 2$. This crudely simulates the contribution to the equatorial zonal wind by the zonal SST gradient (Walker circulation) and meridional SST gradient (Hadley circulation), respectively (see LH for more discussions).

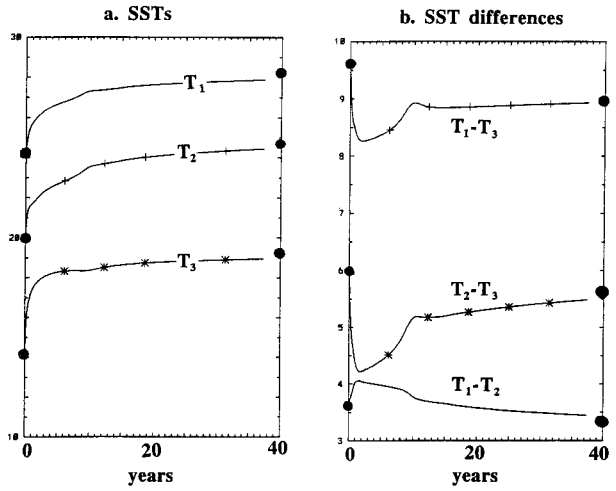

FIG. 6. The response of the OGCM to a sudden onset of global warming (4°C on the equator, 8°C at 50° of latitude). (a) The evolution of the SSTs averaged in the warm pool (T_1), cold tongue (T_2), and the midlatitude (T_3), defined as the spatially averaged SST within (0°, 30°) × (10°S, 10°N), (30°, 60°) × (10°S, 10°N) and (0°, 60°) × (16°N, 36°N), respectively. (b) The evolution of the SST differences. The heavy dots represent the initial and final state after 100 yr. These should be compared with the box model results in Fig. 3.

Similar to the box model run in Fig. 3, an anomalous global warming with a polar amplification is added by increasing the linear restoring SST profile to 39°C (4°C warming) on the equator and −7°C (8°C warming) at 50°. The model is then run for 100 yr after the global warming, when the SST has reached its quasi-steady state. Figure 6a plots the evolution of the SSTs in the warm pool (T_1), cold tongue (T_2), and the midlatitude (T_3), respectively, which are the SSTs spatially averaged within the regions of (0°, 30°) × (10°S, 10°N), (30°, 60°) × (10°S, 10°N), and (0°, 60°) × (16°, 36°N), respectively.

The major features of the box model (Fig. 3) are reproduced in the OGCM experiment. First, all the SSTs experience a warming trend, with the midlatitude SST increasing the fastest, the warm pool SST the second fast, and the cold tongue SST the slowest. This results in two stages of evolution in both the zonal and meridional SST differences (Fig. 6b). The zonal SST contrast increases in the initial 2 yr, consistent with CSCZ, but it decreases toward the final equilibrium state (represented by the heavy dots), consistent with (2.6).

Figures 7a and 7b plot the change of SST after the global warming at year 2 and year 100, respectively. In spite of a simple warming forcing in the restoring SST warming pattern that is independent of longitude, the SST warming pattern is complex even after 100 years due to ocean circulation. The year 2 warming (Fig. 7a) occurs after the surface adjustment stage and is characterized by a maximum in the midlatitude, a submaximum in the warm pool, and a minimum in the cold tongue (and the polar boundary where the mixed layer is deep). This gives an intensified zonal SST gradient and a reduced meridional SST gradient as discussed in the box model (see discussion on Fig. 3). This pattern also resembles qualitatively that of CSCZ in the Tropics. A significantly different pattern emerges in the response of year 100 (Fig. 7b), especially in the Tropics. Now, the cold tongue is warmed about 0.5°C more than in the warm pool, giving a reduced zonal SST gradient. This is reminiscent of the fully coupled CO2 GCM experiments (Knutson and Manabe 1995; Meehl and Washington 1996), although the precise cause of the SST change in these fully coupled GCM experiments has not been identified. In summary, the OGCM ex-

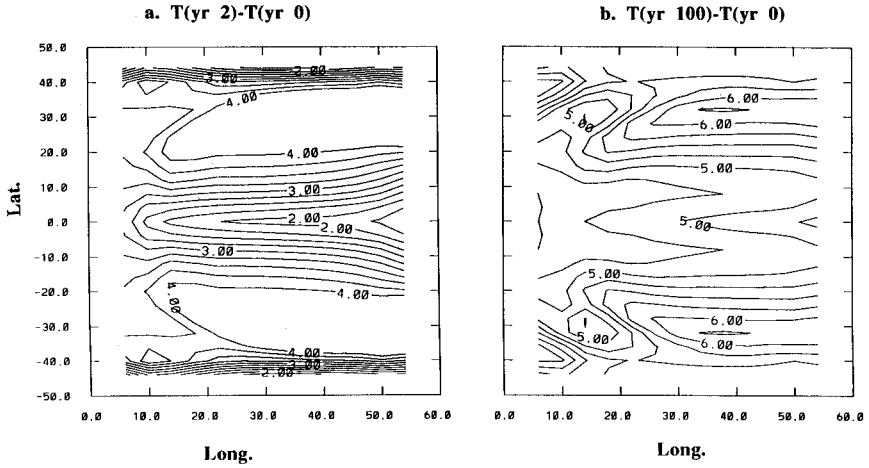

FIG. 7. Two SST anomaly fields (relative to the initial state) in the global warming experiment in Fig. 6. (a) At the end of year 2, (b) at the end of year 100. The initial response in (a) resembles that of Clement et al. (1996) with the warm pool warming faster than the cold tongue. The final response in (b), however, resembles that of Knutson and Manabe (their Fig. 1c) and Meehl and Washington (Fig. 2c), with the cold tongue warming more.

periment supports the major conclusions of our box model study.

4. Summary and discussions

The response of tropical west–east SST contrast to global warming has been studied in a box model and an OGCM. Under a global warming heat flux that does not vary much in space, the transient response of tropical SST to global warming has two distinctive stages. The initial stage is a surface adjustment stage that occurs at interannual timescales. The SST evolution is characterized by a warming weak in the cold tongue, strong in the warm pool, and the strongest in the extratropics. This nonuniform response over different regions results in an increased west–east SST contrast along the equator, as proposed by CSCZ. The later stage is the thermocline adjustment stage, which occurs at the interdecadal timescale. The SST evolves slowly toward its equilibrium response of LH, which depends critically on the nonlocal interaction with the extratropics. The equilibrium west–east SST contrast is determined completely by the latitudinal differential heating, or more precisely, the latitudinal difference of local-equilibrium SST. In addition, the long thermocline memory has been found crucial in producing the characteristics of the transient evolution.

It should be pointed out that our study may not be applied directly to the study of CO_2 increase, mainly because of the neglect of explicit atmospheric processes. What we have studied is simply how the ocean responds to a given surface heat flux forcing. The simple surface heat flux forcing adopted, such as a uniform surface heat flux, is unlikely true in the presence of complex atmospheric processes (Meehl and Washington 1996). Nevertheless, our study does shed light on the role of ocean in the response of tropical climatology to global warming. Several further issues will be discussed below.

a. Effects of high-latitude forcing

The term ''extratropics'' above has been used loosely to refer to the region from which the subduction water can impact the equatorial SST significantly. This region includes most of the eastern part of the subtropical gyre and part of the subpolar gyre. The water in the subtropical gyre can subduct directly due to the downward Ekman pumping (Liu et al. 1994; McCreary and Lu 1994). The water in the subpolar gyre may first penetrate into the subtropical gyre through subpolar–subtropical gyre interaction and then toward the equator.

It seems reasonable to speculate that the effect of climate forcing on equatorial SST tends to decrease away from the Tropics. This speculation is based on two reasonings. First, an anomalous temperature of water at a higher latitude takes a longer time to reach the equator, during which it may lose more heat due to mixing processes. Second, a high-latitude water tends to subduct to a deeper depth in the equatorial thermocline and therefore may be less efficient to affect the SST directly through upwelling.

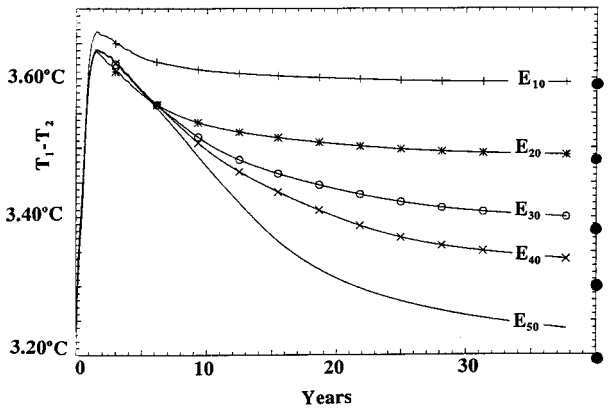

FIG. 8. The time evolution of the zonal SST differences (the same definition as in Fig. 6) of five global warming OGCM experiments of E_{50}, E_{40}, E_{30}, E_{20}, and E_{10}, in which a 4°C global warming is imposed uniformly within the latitude of 50°, 40°, 30°, 20°, and 10°, respectively. The setting of the model is similar to that in Fig. 5, except for a different wind profile that has easterlies in the Tropics and westerlies in the midlatitude (the same as the control run of Liu et al. 1994, see their Fig. 1). The wind curl is zero with 12° of the equator (tropical region), negative from 12° to 32° (subtropical gyre), and positive further poleward (subpolar region). The bold dots represent the $T_1 - T_2$ for each run at the end of year 100.

As a preliminary test for this idea, we performed a series of OGCM experiments with the global warming forcing confined to within different latitude extents. A control run is first carried out with an idealized, yet typical wind field that has tropical easterlies and midlatitude westerlies, as in Liu et al. (1994). The model subtropical and subpolar gyres span from 12° to 32° latitude, and from 32° to the domain boundary at 50°, respectively. A restoring SST is imposed with a constant restoring time of 100 days, and the restoring SST increases linearly from −15°C at 50° to 36°C on the equator. An anomalous global warming is then added on the restoring SST, and the model is run for another 100 yr. Figure 8 plots the initial 40-yr evolution of the zonal SST difference in five experiments: E_{50}, E_{40}, E_{30}, E_{20}, and E_{10}, which have a 4°C warming in restoring SST spatially uniformly within 50°, 40°, 30°, 20°, and 10°, respectively (no warming outside). Since the model domain extends only to 50°, the E_{50} run is a true uniform global warming. The west–east SST difference first increases by about a half degree in the first several years due to the local mechanism of CSCZ and then, as expected from (2.6), decreases to the initial value at about year 100 (heavy dot).

In contrast, the E_{40} run has a global warming only within 40° of latitude, outside of which the SST is still restored toward the original SST. The initial stage of evolution is almost the same as that in E_{50}, but the final state has an increased zonal SST difference of about 0.1°C. The global warming forcing that is applied only

within 40° produces an effective latitudinal differential heating that decreases toward the pole. The final zonal SST difference is therefore increased as in (2.6). Similarly, increases of west–east SST contrast in the final equilibrium state also occur in the other three runs, E_{30}, E_{20}, and E_{10}. However, when the effective meridional differential heating occurs closer to the equator (from 40°, 30°, 20°, to 10° in E_{40}, E_{30}, E_{20}, and E_{10}, respectively), the magnitude of the increased west–east SST difference is enhanced. This confirms our speculation that the equatorial SST is controlled more by the climate forcing that is located closer to the equator.

Two additional points are noteworthy. First, despite the different climate forcing away from the equator, the five runs have the same forcing within 10° of latitude, which corresponds to virtually identical initial responses of increased west–east SST contrast. This therefore demonstrates clearly that the mechanism of CSCZ is a local mechanism that depends only on local tropical climate forcing.

Second, even though the effect of climate forcing decreases toward the pole, a climate forcing anomaly as far as the subpolar gyre (say E_{40} here) can still be important on tropical SSTs. This is not inconsistent with tracer observations, which have identified source waters for the lower equatorial thermocline as far as the Antarctic Circumpolar Current in the Southern Pacific (Toggweiler et al. 1989). This high-latitude effect may also provide another mechanism for the enhanced west–east SST contrast in the experiment in Fig. 2. Seager and Murtugudde have used a restoring boundary of temperature outside 40° of latitude. This restoring, together with the uniform surface heat flux within 40° of latitude, effectively provides an enhanced latitudinal differential heating and in turn the west–east SST contrast in the final steady state.

b. Dynamic ocean–atmosphere coupling

It has been suggested that the ocean–atmosphere dynamic coupling between the wind and upwelling can further increase the west–east SST contrast (CSCZ; Meehl and Washington 1996; SM; Cane et al. 1997). The argument is that a stronger coupling produces both a stronger upwelling transport and a colder upwelling water, both being in favor of a colder cold tongue. However, it is not obvious if the west–east SST gradient will always be strengthened, although the increased cold upwelling can obviously regulate the warming of tropical SST. Indeed, when the coupling reaches the intensity such that the ocean advective timescale is comparable to that of surface radiative time in the Tropics (a year or so), the coupled system reaches a saturation state in which the west–east SST contrast will no longer increase with the coupling. If this is true for the present Pacific [which is likely as argued by LH and Liu (1997)], an increase of dynamic coupling will no longer increase the west–east SST contrast. This has been confirmed in our experiments with idealized box as well as OGCM studies (Fig. 5 is indeed one example in the presence of dynamic coupling).

c. The reduction of west–east SST contrast in coupled GCMs

Almost all the fully coupled models with CO_2 increase show a reduction of the west–east SST difference. The mechanisms for the reduction, however, can be complex. In the fully coupled model of Knutson and Manabe (1995), the reduction of the zonal SST difference is thought to be caused by the strongly nonlinear temperature–evaporation feedback. This seems to be also true in an experiment with an AGCM coupled to a slab mixed layer (with Q-flux correction) (T. R. Knutson 1996, personal communication). In addition, results from fully coupled models and AGCMs that are coupled with a slab mixed layer (Meehl and Washington 1986, 1989, 1996; Oglesby and Saltzman 1992; Washington and Meehl 1993) also suggest the cloud-albedo feedback as an important mechanism. All these works have emphasized the role of the atmospheric processes.

Here, we can also give a possible mechanism from the oceanic pespective. In almost all the fully coupled models, the SST tends to be warmed up more in the middle and high latitude than in the Tropics (or the so-called polar amplification, which, nevertheless, seems to be absent in observations). This indicates a larger warming in the extratropics and in turn a reduction of latitudinal differential heating. The west–east SST contrast therefore should be reduced after thermocline adjustment as discussed regarding Figs. 3, 6, and 7.

Finally, a more fundamental question is why the response of west–east SST contrast seems to be opposite to recent observational analyses, which tend to show an increased SST contrast in the central equatorial Pacific (Cane et al. 1997; Kaplan et al. 1998; Latif et al. 1997). It is possible that observations have substantial errors, especially in the early half of the century when the data are extremely poor. It is also possible that some fundamental elements are missing in current generations of coupled GCMs. The separation of natural interdecadal variability can also further complicate the picture in both observations and models. As far as the mechanism is concerned, most of the known mechanisms in the atmosphere, such as the temperature–evaporation feedback, the cloud–albedo feedback, and atmospheric circulation, tend to give a reduced west–east SST contrast in the presence of a global warming. There are, however, at present, two mechanisms to produce an increased west–east SST contrast: the local and transient mechanism of CSCZ and the nonlocal and equilibrium mechanism that is discussed in section 2. Both mechanisms involve oceanic processes. This indicates that the ocean may play an important role in the response of tropical climatology to a global warming.

Acknowledgments. This work is strongly motivated by discussions with Dr. R. Seager, Ms. A. Clement, and Dr. M. Cane. This work has also benefited from discussions and comments from Drs. T. Knutson, R. Oglesby, D. Gu, G. Meehl, S. Manabe, R. Miller, and the two anonymous reviewers. The OGCM experiments are performed by Mr. Boyin Huang. This work is supported by NSF and NOAA.

APPENDIX A

Transient Response to a General Climate Forcing

Most of the features of the transient response can also be studied analytically in the box model. For convenience, we only study the response to a spatially uniform global warming $T_E = T_M = H$ in (2.5) (and denote m/τ_3 as m). At timescales longer than that of surface relaxation and advection (or $d/d\tau \ll 1$), the evolution of the SSTs are determined mainly by the quasi-equilibrium balance between the surface heat flux and the advection. Equations (2.5) can then be approximated as

$$0 = H - T_1 + q(T_2 - T_1), \tag{A.1a}$$

$$0 = H - T_2 + q(T_4 - T_2), \tag{A.1b}$$

$$0 = m(H - T_3) + q(T_1 - T_3), \tag{A.1c}$$

$$MdT_4/d\tau = q(T_3 - T_4). \tag{A.1d}$$

The temporal evolution of the climate is forced by that of the surface forcing, while the memory is provided entirely by the subsurface water M. The surface heat balances of (A.1a)–(A.1c) give the relationships

$$T_1 - T_2 = (H - T_4)q(m + q)/A, \tag{A.2a}$$

$$T_1 - T_3 = -(H - T_4)mq^2/A, \tag{A.2b}$$

$$T_2 - T_3 = -(H - T_4)q[m(1 + q) + q]/A, \tag{A.2c}$$

$$T_3 - T_4 = (H - T_4)\{[(m + 1)q + m] \times (1 + q) + q^2\}/A, \tag{A.2d}$$

where $A = (1 + q)^2(m + q)$. If the climate forcing is steady (or has a timescale much longer than the thermocline adjustment), the thermocline heat budget equation (A.1d) gives the forced steady-state response $T_4 = T_3$, and then (A.2d) leads to $H - T_4 = 0$. Thus, (A.2a)–(A.2c) give uniform global warming $T_1 = T_2 = T_3 = T_4 = H$.

If the climate forcing $H(\tau)$ varies with time, the uniform global response will not occur. This is because the finite memory of the thermocline delays the response of the thermocline temperature from the surface forcing and therefore $H(\tau) - T_4(\tau) \neq 0$. The evolution of the SST gradients in (A.1a)–(A.1c) then yield

$$T_1(\tau) - T_2(\tau) \sim H(\tau) - T_4(\tau) \sim -[T_1(\tau) - T_3(\tau)],\ -[T_2(\tau) - T_3(\tau)].$$

Thus, the SST gradients are always negatively correlated between the zonal and meridional directions. This has been seen in Figs. 3, 4, 5, and 6.

The critical role of the subsurface memory also becomes clear. For a small subsurface memory $M \to 0$, (A.1d) gives $T_3 = T_4$, even in the presence of a temporally varying climate forcing. Therefore, (A2) gives a globally uniform variation of the ocean temperature: $T_1(\tau) = T_2(\tau) = T_3(\tau) = T_4(\tau) = H(\tau)$. Obviously, the small subsurface water mass enables the subsurface to adjust rapidly to the surface forcing and therefore damps the temperature anomalies that are not in phase with the surface forcing, as discussed in Fig. 4.

APPENDIX B

Amplitude and Timescale of the Response

For a perturbation climate forcing of $\delta T_E = \delta T_M = he^{i\sigma\tau}$, the response of the temperature anomalies have the form $T_n = t_n e^{i\sigma\tau}$ ($n = 1, 2, 3, 4$). Using (A.1), one can derive the temperature differences as

$$t_1 - t_2 = hBq/(1 + q)^2, \tag{B.1a}$$

$$t_1 - t_3 = -hBmq^2/[(1 + q)^2(m + q)], \tag{B.1b}$$

$$t_2 - t_3 = -hBq[m(1 + q) + q]/[(1 + q)^2(m + q)], \tag{B.1c}$$

where

$$B = i\sigma M/(bq + i\sigma M), \tag{B.2}$$

and $b = [m(1 + q)^2 + q(1 + 2q)]/[(1 + q)^2(m + q)] > 0$. Thus, (B.2) and (B.1a)–(B.1c) show that the amplitude of the SST differences increases with the subsurface memory, M, as seen in Fig. 4.

Furthermore, the amplitude also varies with the mean transport q. For either a weak ($q \to 0$) or a strong ($q \to \infty$) transport, we have the uniform surface response $t_1 = t_2 = t_3 = h$. The former is caused by a pure local response, while the latter by a too strong heat transport. (Yet notice that, in the former case, there is no thermocline variability $t_4 = 0$, while in the latter case, the thermocline temperature responds the same as the SSTs, $t_4 = h$.) As a result, the transient response reaches its maximum amplitude, or saturation level, at a finite transport of $q \sim O(1)$, when the surface advection timescale is comparable to that of the surface relaxation. The mechanism for the saturation of the amplitude of the transient response is essentially the same as that for the saturation in the steady state [see (2.7), and LH]. Indeed, with $M \to \infty$, we have from (B.1) $t_1 - t_2 \to hq/(1 + q)^2 \leq h/4$; $t_1 - t_3 \to h$, $t_2 - t_3 \to h$. Therefore, the upper bound is a quarter of that of the thermal forcing for the zonal SST difference but can reach the thermal forcing itself for the meridional SST difference. These are exactly the same as the steady-state response to a latitudinal differential heating in LH. Physically, the

spatial variability of SST can be produced by either a spatially varying heating as in LH or a transient forcing that is spatially uniform as here. It is therefore not unexpected that the amplitude of the two responses shares the same saturation feature.

Finally, the timescale for the subsurface adjustment stage can also be estimated. Assuming the absence of the thermal forcing $H = 0$, and substitute $T_n = t_n e^{i\sigma t}$ into (A1), one can solve the eigenvalue problem to give the damping as

$$i\sigma = -(1/M) \times q[(2 + m)q^2 + (1 + 2m)q + m] \div [(1 + q)^2(m + q)] < 0.$$

This damped mode represents the negative thermocline feedback. The damping timescale is determined by both the thermocline water mass and the transport. A small subsurface memory ($M \to 0$) gives a short damping time or a strong damping, consistent with Fig. 4. As a result, the response to a uniform global warming is also spatially uniform. In the limit of a strong transport ($q \to \infty$), the damping timescale approaches a finite limit of $-(2 + m)/M$. For a weaker transport ($q \to 0$), however, the damping timescale approaches infinite, indicating a weaker damping or longer adjustment time. Thus, unlike the amplitude, the adjustment timescale decreases monotonically with the transport.

REFERENCES

Bretherton, F., 1982: Ocean climate modeling. *Progress in Oceanography,* Vol. 46, Pergamon, 2621–2624.

Cane, M. A., A. C. Clement, A. Kaplan, Y. Kushnir, D. Pozdnyakov, R. Seager, and S. Zebiak, 1997: Twentieth century sea surface temperature trends. *Science,* **275**, 957–960.

Clement, A. C., R. Seager, M. A. Cane, and S. E. Zebiak, 1996: An ocean dynamic thermostat. *J. Climate,* **9,** 2190–2196.

Dijkstra, H. A., and J. D. Neelin, 1995: Ocean–atmosphere interaction and the tropical climatology: Part II: Why the Pacific cold tongue is in the east. *J. Climate,* **8,** 1343–1359.

Fu, R., A. D. del Genio, W. B. Rossow, and W. T. Liu, 1992: Cirrus-cloud thermostat for tropical sea surface temperature tested using satellite data. *Nature,* **358,** 394–397.

Hartmann, D., and M. Michelsen, 1993: Large-scale effects on the regulation of tropical sea surface temperature. *J. Climate,* **6,** 2049–2062.

Kaplan, A., M. Cane, Y. Kushnir, A. Clement, B. Blumenthal, and B. Rajagopalan, 1998: Analyses of global sea surface temperature 1856–1991. *J. Geophys. Res.,* in press.

Knutson, T. R., and S. Manabe, 1995: Time-mean response over the tropical Pacific to increased CO_2 in a coupled ocean–atmosphere model. *J. Climate,* **8,** 2181–2199.

Latif, M., R. Kleeman, and C. Eckert, 1997: Greenhouse warming, decadal variability, or El Niño? An attempt to understand the anomalous 1990s. *J. Climate,* **10,** 2221–2239.

Lau, N.-C., and M. J. Nath, 1996: The role of ''atmospheric bridge'' in linking tropical Pacific ENSO events to extratropical SST anomalies. *J. Climate,* **9,** 2036–2057.

Liu, Z., 1994: A simple model of the mass exchange between the subtropical and tropical ocean. *J. Phys. Oceanogr.,* **24,** 1153–1165.

——, 1997: Oceanic regulation of the atmospheric Walker circulation. *Bull. Amer. Meteor. Soc.,* **78,** 407–413.

——, and B. Huang, 1997: A coupled theory of tropical climatology: Warm pool, cold tongue, and Walker circulation. *J. Climate,* **10,** 1662–1679.

——, S. G. H. Philander, and R. Pacanowski, 1994: A GCM study of tropical-subtropical thermocline circulation in the upper ocean. *J. Phys. Oceanogr.,* **24,** 2606–2623.

McCreary, J., and P. Lu, 1994: On the interaction between the subtropical and the equatorial oceans: The subtropical cell. *J. Phys. Oceanogr.,* **24,** 466–497.

Meehl, G. A., and W. M. Washington, 1986: Tropical response to increased CO_2 in a GCM with a simple mixed layer ocean: Similarities to an observed Pacific warm event. *Mon. Wea. Rev.,* **114,** 667–674.

——, and ——, 1989: Climate sensitivity due to increased CO_2: Experiments with a coupled atmosphere and ocean general circulation model. *Climate Dyn.,* **4,** 1–38.

——, and ——, 1996: El Niño-like climate change in a model with increased atmospheric CO_2 concentrations. *Nature,* **382,** 56–60.

Miller, R. L., 1997: Tropical thermostats and low cloud cover. *J. Climate,* **10,** 409–440.

Neelin, J. D., and H. A. Dijkstra, 1995: Ocean–atmosphere interaction and the tropical climatology: Part I: The dangers of flux correction. *J. Climate,* **8,** 1325–1342.

Oglesby, R. J., and B. Saltzman, 1992: Equilibrium climate statistics of a general circulation model as a function of atmospheric carbon dioxide. Part I: Geographic distributions of primary variables. *J. Climate,* **5,** 66–92.

Pierrehumbert, R. T., 1995: Thermostats, radiator fins, and the local runaway greenhouse. *J. Atmos. Sci.,* **52,** 1784–1806.

Ramanathan, V., and W. Collins, 1991: Thermodynamic regulation of ocean warming by cirrus clouds deduced from observations of the 1987 El Nino. *Nature,* **351,** 27–32.

Seager, R., and R. Murtugudde, 1997: Ocean dynamics, thermocline adjustment and regulation of tropical SST. *J. Climate,* **10,** 521–534.

——, Y. Kushnir, and M. A. Cane, 1995: On heat flux boundary conditions for ocean models. *J. Phys. Oceanogr.,* **25,** 3219–3230.

Sun, D., and Z. Liu, 1996: Dynamic ocean–atmosphere coupling: A thermostat for the tropics. *Science,* **272,** 1148–1150.

Toggweiler, R., K. Dixon, and W. S. Broecker, 1989: The Peru upwelling and the ventilation of the South Pacific thermocline. *J. Geophys. Res.,* **96,** 20 467–20 497.

Waliser, D., 1996: Formation and limiting mechanisms for very high sea surface temperature: Linking the dynamics and thermodynamics. *J. Climate,* **9,** 161–188.

Wallace, J. M., 1992: Effect of deep convection on the regulation of tropical sea surface temperature. *Nature,* **357,** 230–231.

Washington, W. M., and G. A. Meehl, 1993: Greenhouse sensitivity experiments with penetrative cumulus convection and tropical cirrus albedo effects. *Climate Dyn.,* **8,** 211–223.